

Development of New Flexible Lifetime Model: its Associated Inferences and Applications to Cancer and Covid-19 Data

Samuel Adewale Aderoju (1, *)
Kazeem Adesina Dauda (1,2)
Julius Babatunde Olaifa (1)

Received: 24/03/2025
Revised: 16/04/2025
Accepted: 17/04/2025

© 2025 University of Science and Technology, Aden, Yemen. This article can be distributed under the terms of the [Creative Commons Attribution License](#), which permits unrestricted use, distribution, and reproduction in any medium, provided the original author and source are credited.

© 2025 جامعة العلوم والتكنولوجيا، المركز الرئيس عدن، اليمن. يمكن إعادة استخدام المادة المنشورة حسب رخصة مؤسسة المشاع الإبداعي شريطة الاستشهاد بالمؤلف والمجلة.

¹ Department of Mathematics and Statistics, Kwara State University, Malate, Nigeria

² Department of Mathematics, University of Bergen, 5007 Bergen, Norway

*Corresponding Author's Email: samuel.aderoju@kwasu.edu.ng

Development of New Flexible Lifetime Model: its Associated Inferences and Applications to Cancer and Covid-19 Data

Samuel Adewale Aderoju

*Department of Mathematics and
Statistics, Kwara State University, Malate,
Nigeria*

samuel.aderoju@kwasu.edu.ng

Kazeem Adesina Dauda

*Department of Mathematics and
Statistics, Kwara State University, Malate,
Nigeria,*

*Department of Mathematics, University
of Bergen, 5007 Bergen, Norway*

Julius Babatunde Olaifa

*Department of Mathematics and
Statistics, Kwara State University,
Malate, Nigeria*

Abstract— In this paper, a New Two-Parameter Generalized Lindley Distribution (NTGLD) for modelling lifetime data is proposed, which is designed to enhance the flexibility and applicability of the Lindley distribution in real data analysis. Key statistical properties such as the first four moments about the origin, coefficient of variation, hazard and survival functions of the NTGLD are equally obtained. The parameters of the NTGLD were estimated using the method of maximum likelihood. A comprehensive simulation study compares the efficiency of the estimators is presented. The quantile plot provides further insights, illustrating how the distribution's quantile varies with the parameters α and θ , emphasizing the adaptability of the model to different data structures. The NTGLD is applied to three real datasets: remission times of 128 bladder cancer patients, remission times of 36 bladder cancer patients, and recovery times of 553 Covid-19 patients. In each case, the NTGLD demonstrates superior fit compared to competing models considered in this study. Performance metrics such as Akaike Information Criteria, Akaike Information Criteria Corrected, Hannan–Quinn information criteria and Bayesian Information Criteria consistently favour the NTGLD, underscoring its robustness and effectiveness. This study establishes the NTGLD as a valuable tool for statistical modelling, offering significant improvements over existing distributions considered in terms of flexibility, accuracy, and fit.

Keywords— Generalized Lindley Distribution; Maximum Likelihood Estimation; Quantile Plot; Simulation Study; Covid-19 Data; Cancer Data

I. INTRODUCTION

To date, researchers have developed and are still developing distributions to enhance the analysis and interpretation of lifetime data sets. These distributions are crucial for gaining deeper insights into real-world phenomena. Notably, the methods for constructing new probability distributions have evolved significantly since 1997. The primary goal of developing, extending, or generalizing these distributions is to better explain lifetime phenomena across various fields, such as public health, engineering, and biological sciences [1]. Lifetime distributions, alternatively known as survival distributions or failure time distributions, serve as a cornerstone statistical framework for modeling the time until a specific event occurs [2], [3], [4], and [5]. Traditional distributions like uniform, beta, exponential, Rayleigh, Weibull, and gamma have limited flexibility. For instance, the exponential distribution is tied to a constant hazard function, and the Rayleigh distribution is constrained to increasing hazard functions. The Weibull distribution offers more flexibility, supporting increasing, decreasing, or constant hazard functions, but it

cannot model non-monotonic failure rates, such as those with unimodal or bathtub shapes [1]. New distributions generated from emerging families and other probability distribution generators have gained significant attention in the literature due to their flexibility and stability [6]. Johnson et al. [7] and [8] have provided comprehensive reviews of hundreds of continuous univariate distributions. Gomes-Silva et al. [9] noted that recent research has focused more on developing new families of distributions that extend established ones, offering greater flexibility in modeling lifetime data. Similarly, Taketomi et al. [10] conducted an extensive review of parametric distributions used in lifetime models.

Despite the wide-ranging applications of the Lindley distribution [11], it falls short in adequately modeling phenomena characterized by non-monotone failure rates, such as bathtub-shaped or upside-down failure rates. Consequently, many researchers have introduced new generalizations of the traditional Lindley distribution by incorporating one or more shape parameters to enhance the flexibility of both the probability density function (PDF) and the hazard rate function. Some of such significant advancements are the generalized Lindley distribution by Zakerzadeh and Dolati [12], a new class of generalized Lindley distributions introduced by Oluyede and Yang [13], a generalized Lindley distribution with shape considerations presented by Nadarajah et al. [14], the quasi-Lindley distributions (QLD) introduced by Shanker and Mishra [15], and a new generalized Lindley distribution by Abouammoh et al. [16]. In recent years, many probability distributions, such as Lindley, Rayleigh, exponential, Weibull, and gamma, among others, have been extended and applied in statistical analysis for modeling lifetime data. Many researchers used these distributions in different areas of applicability. For instance, Al-Noor and Assi [17] developed a Rayleigh-Rayleigh model with an increasing failure rate and applied it to real-life data and a simulation study. The results of its application to real-life data show that the distribution produced fits that are competitive and compare better, in some cases, to the gamma, Weibull, and lognormal distributions.

Therefore, the literature has seen the development of several extensions and applications of well-established distributions. For example, a one-parameter distribution called the Pranav distribution was proposed by Shukla [18]. The distribution is a mixture of exponential distribution with scale parameter θ and gamma distribution with shape parameter and scale parameter θ . Aderoju [19] introduced the Samade

distribution, which was subsequently extended by Aderoju & Babaniyi [20] and Elangovan & Manivasagan [21]. The Samade distribution has been widely used for modeling survival, reliability data, and its mixture for modeling count data [22], [23]. Hosseini et al. [24] introduced a new one-parameter weighted-Lindley distribution for modeling lifetime data. They derived and investigated some of its basic properties. The application of the model to a real dataset was done to investigate the flexibility of the new weighted-Lindley distribution as compared with other distributions. Meriem et al. [25] introduced the power XLindley (PXL) distribution, a two-parameter extension of the XLindley distribution. Aderoju and Jolayemi [26] explored extensions of the Hamza distribution, which features a unique failure rate function that enhances its applicability in modeling real-world scenarios. Aleshinloye et al. [27] proposed a New Generalized Gamma-Weibull Distribution, while Aderoju and Adeniyi [28] investigated extensions of the Generalized Akash distribution. Tashkandy *et al.* [29] introduced a novel two-parameter distribution called the power-modified XLindley distribution. They developed it through the application of power transformation techniques to the existing modified XLindley distribution [30]. They conducted a thorough examination of its statistical properties, exploring its potential to improve data fitting and modeling accuracy. Aderoju et al. [31] introduced a new three-parameter Weibull-generalized gamma distribution, which provides more flexibility in modeling lifetime data. The results of the model's simulation and application to real-life data suggest that it is a useful alternative to the existing distributions considered in the paper.

The primary objective of this article is to present a new flexible lifetime distribution and some of its characteristics. The distribution is capable of being used in survival analysis of patients suffering from diseases such as cancer, Covid-19, tuberculosis, etc., and can also be used to model the volatility of organic molecules that are relevant to environmental studies. Essentially, a major motivation for this study is to demonstrate that the proposed distribution has the potential to model medical data. In terms of application, the scope of this study is non-censored data, and a simulation study is also involved.

The following is the order of this article. We introduce the new lifetime distribution called a new two-parameter generalized Lindley (NTGL) distribution in Section 2. The mathematical properties of the NTGL distribution are presented in Section 3. The parameter estimation of the NTGL distribution and simulation study are covered in

Section 4. The application to real data analysis is analyzed in Section 5. The conclusions are provided in Section 6.

II. MATERIAL AND METHOD

The new two-parameter generalized Lindley (NTGL) distribution, characterized by the parameters α and θ , is defined through its probability density function (PDF). This PDF follows the general structure of a k -component additive mixture distribution, as outlined by Everitt and Hand [32]. Specifically, for a random variable x , the PDF is given by:

$$f(x, \theta) = \sum_{j=1}^k p_j f_j(x, \theta_j), \quad (1)$$

where θ_j is the vector of parameters for the mixture models, p_j is the mixture proportion and $\sum_{j=1}^k p_j = 1$.

Definition: A random variable X with a PDF representing the two-parameter generalized Lindley distribution is expressed as:

$$f(x; \alpha, \theta) = \frac{\theta^2}{4 + \theta^2} \left(\theta + \frac{4x^{\alpha-2} \theta^{\alpha-3}}{\Gamma(\alpha-1)} \right) e^{-\theta x}, \quad x, \theta > 0, \alpha > 1 \quad (1)$$

Remark: The PDF (1) can be shown as a mixture of exponential (θ) and gamma ($\alpha - 1, \theta$) distributions as follows:

$$f(x; \alpha, \theta) = p g_1(x; \theta) + (1 - p) g_2(x; \alpha - 1, \theta),$$

where

$$p = \frac{\theta^2}{\theta^2 + 4}, \text{ is the mixing proportion (or mixture weight),}$$

$$g_1(x; \theta) = \theta e^{-x\theta}, \quad x > 0$$

and

$$g_2(x; \alpha - 1, \theta) = \frac{\theta^{\alpha-1} x^{\alpha-2}}{\Gamma(\alpha-1)} e^{-x\theta}, \quad x, \theta > 0, \alpha > 1.$$

We arbitrarily use $X \sim NTGL(\alpha, \theta)$ to denote the random variable having new two-parameter generalized Lindley distribution with parameters α (shape) and θ (rate) with PDF (1). The probability density curves for some selected values of the shape and scale parameters are presented in Figure 1.

The probability density curves for some selected values of the shape and scale parameters are presented in Figure 1. Some of the curves in this Figure 1 revealed a bimodal distribution, and since the new distribution consists of both exponential and gamma components, our developed methods are well-suited to account for this bimodality if present in the lifetime data, like this simulation scenario.

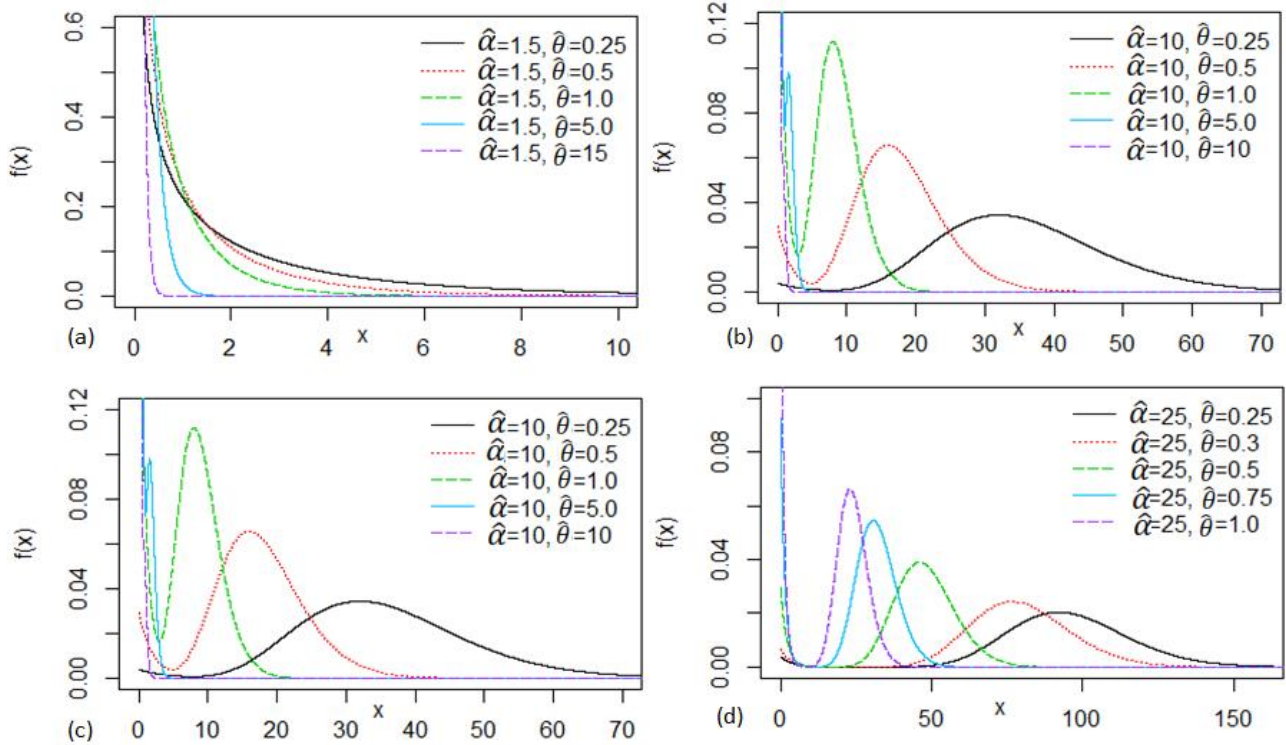


Figure 1: Shape of the NTGL distribution for different values of the parameters

Figure 2 represents the image of a 3D surface plot generated in R, showing the PDF of the NTGL distribution at a fixed value $x = 5$. The plot illustrates how the PDF changes with varying values of the parameters α and θ . Note that X-axis represents the parameter α , ranging from 1.5 to 3, while Y-axis Represents the parameter θ , ranging from 0.5 to 2, and the Z-axis Represents the value of the PDF, ranging from approximately 0 to 0.25. The surface indicates the PDF values corresponding to different combinations of α and θ . The shape

of the surface provides insights into how the PDF of the NTGL distribution behaves with changes in these parameters. The plot shows that as α increases, the PDF value increases significantly, especially for larger values of θ . The color gradient on the right side of the plot provides a visual representation of the PDF values: Darker colors represent higher PDF values, while lighter colors represent lower PDF values. Figures 3 illustrates the cdf of the NTGL distribution for various values of the parameters.

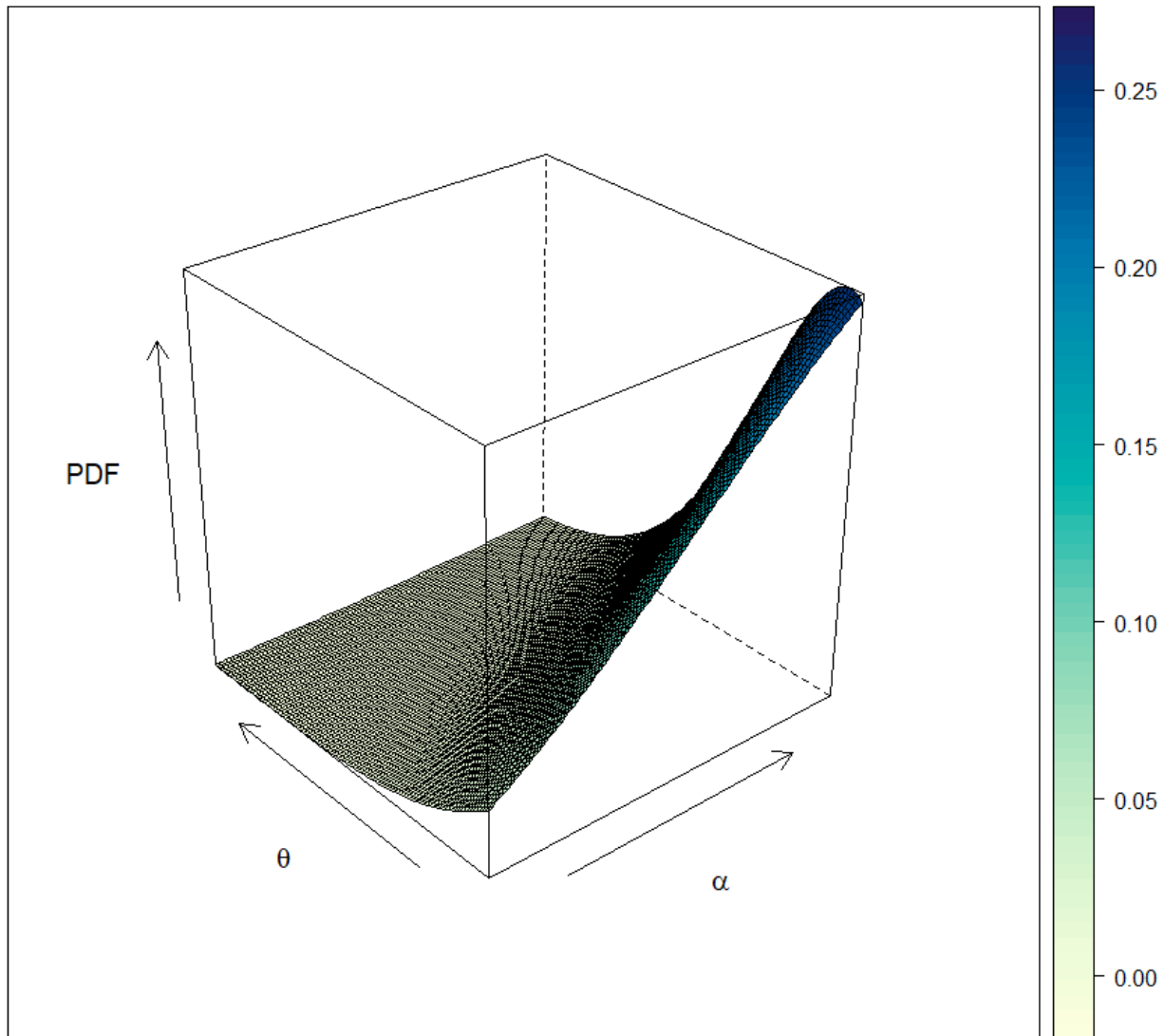


Figure 2: The 3D surface plot of the PDF of the NTGL distribution at a fixed value $x = 5$

The corresponding cumulative distribution function (cdf) can be obtained as follows:

$$\begin{aligned}
 F(x; \alpha, \theta) &= \int_0^x f(t; \alpha, \theta) dt \\
 &= \int_0^x \frac{\theta^2}{4 + \theta^2} \left(\theta + \frac{4t^{\alpha-2}\theta^{\alpha-3}}{\Gamma(\alpha-1)} \right) e^{-\theta t} dt \\
 &= \frac{\theta^2}{4 + \theta^2} \left[\int_0^x (\theta e^{-\theta t}) dt \right. \\
 &\quad \left. + \int_0^x \left(\frac{4t^{\alpha-2}\theta^{\alpha-3}}{\Gamma(\alpha-1)} e^{-\theta t} \right) dt \right] \\
 &= \frac{\theta^2}{4 + \theta^2} \left[(1 - e^{-x\theta}) + \frac{4\Gamma(\alpha-1, x\theta)}{\theta^2\Gamma(\alpha-1)} \right]
 \end{aligned}$$

$$= \frac{\theta^2}{4 + \theta^2} (1 - e^{-x\theta}) + \frac{4\theta^{\alpha-1}\Upsilon(\alpha-1, \theta x)}{(4 + \theta^2)\Gamma(\alpha-1)}$$

Therefore,

$$\begin{aligned}
 F(x|\alpha, \theta) &= \frac{1}{4 + \theta^2} \left(\theta^2(1 - e^{-\theta x}) \right. \\
 &\quad \left. + \frac{4\theta^{\alpha-1}\Upsilon(\alpha-1, \theta x)}{\Gamma(\alpha-1)} \right) \quad (2)
 \end{aligned}$$

The cdf for some selected values of the shape and scale parameters are presented in Figure 2; where $\Upsilon(\cdot)$ incomplete gamma function. These cdf plots illustrate the flexibility of the NTGLD in modeling distributions that can either concentrate around lower values or spread across a broader range, depending on the parameters α and θ .

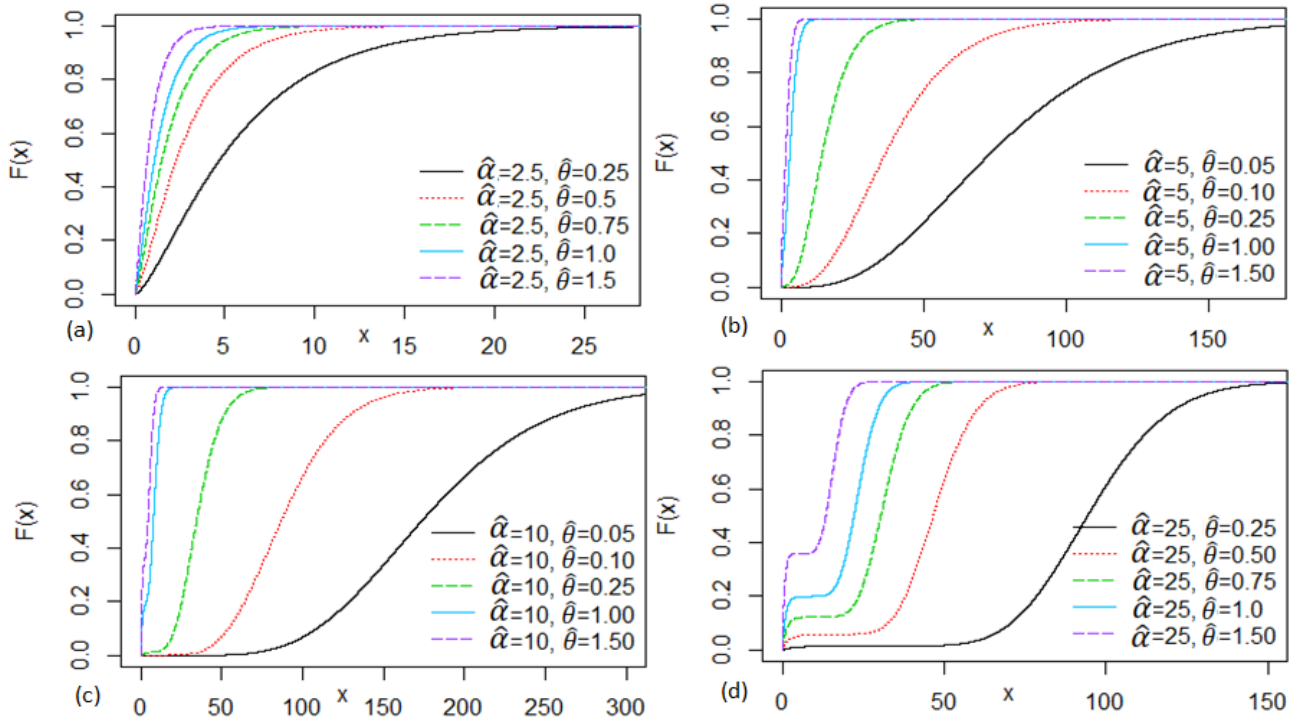


Figure 3: CDF curves of the NTGL distribution for some selected values of parameters.

[III] MATHEMATICAL PROPERTIES OF THE NTGL DISTRIBUTION

Using algebraic expressions to ascertain some mathematical characteristics can prove more advantageous compared to direct computation through numerical methods. Hence, we proceed to introduce some mathematical properties of the NTGL distribution.

Asymptotic Behaviour

This subsection discusses the behaviour and probable shapes features of the PDF of NTGL distribution. The PDF's behaviour is as follows:

$$\lim_{x \rightarrow 0} f(x) = \begin{cases} \rightarrow \infty, & \text{if } 1 < \alpha < 2 \\ \frac{\theta(\theta^2 + 4)}{4 + \theta^2}, & \text{if } \alpha = 2 \\ \frac{\theta^3}{4 + \theta^2}, & \text{if } \alpha > 2 \end{cases}$$

Moments and Associated Measures

The r th factorial moment

Moments of a given density function are very useful in computing measures of central tendency, variance, skewness, and kurtosis. Using equation (1), the r th factorial moment of the random variable X (said to be following the NTGL distribution) about the origin is obtained as:

$$\begin{aligned} E(X^r) &= \mu_r = \int_0^{\infty} x^r f(x|\alpha, \theta) dx \\ \mu_r &= \int_0^{\infty} x^r \frac{\theta^2}{4 + \theta^2} \left(\theta + \frac{4x^{\alpha-2}\theta^{\alpha-3}}{\Gamma(\alpha-1)} \right) e^{-\theta x} dx \\ &= \frac{\theta^2}{4 + \theta^2} \int_0^{\infty} x^r \left(\theta + \frac{4x^{\alpha-2}\theta^{\alpha-3}}{\Gamma(\alpha-1)} \right) e^{-\theta x} dx \end{aligned}$$

The final expression of ordinary moments is given in the following form:

$$\mu'_r = \frac{\theta^2 \Gamma(1+r) \Gamma(\alpha-1) + 4 \Gamma(r+\alpha-1)}{\theta^r (4 + \theta^2) \Gamma(\alpha-1)} \quad (3)$$

The initial four moments of the random variable X , about the origin, are derived from equation (3) by substituting r with values of 1, 2, 3, and 4 respectively.

$$\begin{aligned} \mu'_1 &= \frac{4(\alpha-1) + \theta^2}{\theta(4 + \theta^2)} \\ \mu'_2 &= \frac{2(\theta^2 + 2\alpha(\alpha-1))}{\theta^2(4 + \theta^2)} \\ \mu'_3 &= \frac{4\alpha^3 - 4\alpha + 6\theta^2}{\theta^3(4 + \theta^2)} \\ \mu'_4 &= \frac{4((\alpha-1)\alpha(1+\alpha)(2+\alpha) + 6\theta^2)}{\theta^4(4 + \theta^2)} \end{aligned}$$

The variance (σ^2), coefficient of variation (CV), the index of dispersion (ID), coefficient of skewness (S_k) and coefficient of Kurtosis (K_s) are obtained as:

$$\begin{aligned} \sigma^2 &= E(X^2) - [E(X^1)]^2 = \mu_2 - [\mu_1]^2 \\ \sigma^2 &= \frac{\theta^4 + 4\alpha^2\theta^2 + 16\theta^2 - 16 - 4\alpha(3\theta^2 - 4)}{\theta^2(4 + \theta^2)^2} \end{aligned}$$

$$\begin{aligned} CV &= \frac{\sigma}{\mu_1} \\ CV &= \frac{\sqrt{(16(\theta^2 + \alpha - 1) - 12\alpha\theta^2 + 4\alpha^2\theta^2 + \theta^4)}}{(\theta^2 + 4\alpha - 4)(4\theta + \theta^3)} \end{aligned}$$

$$S_k = \frac{\mu'_3}{\sigma^3}$$

$$S_k = \frac{6\theta^2 - 4\alpha + 4\alpha^3}{\theta^3(4 + \theta^2) \left(\frac{16(\theta^2 - 1) + 4\alpha^2\theta^2 + \theta^4 - 4\alpha(-4 + 3\theta^2)}{\theta^2(4 + \theta^2)^2} \right)^{3/2}} = \frac{16(\theta^2 + \alpha - 1) + \theta^2(\theta^2 + 4\alpha^2 - 12\alpha)}{(\theta^2 + 4\alpha - 4)(\theta^3 + 4\theta)}$$

$$K_s = \frac{\mu_4'}{\sigma^4} = \frac{4(4 + \theta^2)^3((\alpha - 1)\alpha(1 + \alpha)(2 + \alpha) + 6\theta^2)}{(16(\theta^2 - 1) + 4\alpha^2\theta^2 + \theta^4 - 4\alpha(3\theta^2 - 4))^2}$$

$$ID = \frac{\sigma^2}{\mu_1} = \frac{16(\theta^2 + \alpha - 1) - 12\alpha\theta^2 + 4\alpha^2\theta^2 + \theta^4}{(-4 + 4\alpha + \theta^2)(4\theta + \theta^3)}$$

Table 1 provides key statistical measures numerically for the NTGL distribution across different values of the parameters α and θ . As α increases, all the measures (mean, variance, skewness, and kurtosis) show significant increases, especially for small values of θ . This indicates that for large α , the distribution becomes more dispersed, more skewed, and more kurtotic, with fatter tails. For increasing θ , the measures (especially variance, skewness, and kurtosis) decrease, implying that the distribution becomes more symmetric and less spread out, with lighter tails.

Table 1: Numerical description of certain key measures of the NTGL distribution

Parameters	Measures					
	θ	μ	σ^2	ID	S_k	K_s
$\alpha = 1.25$	0.05	5.0093	100.32	20.028	5.6237	36.5395
	0.25	1.0461	3.3209	4.1303	5.5907	35.9133
	0.50	0.5882	1.3010	2.2117	5.4700	33.6740
	1.00	0.4000	0.4900	1.2250	5.1384	27.6056
	5.00	0.1793	0.0385	0.2149	5.5721	22.6294
	10.0	0.0971	0.0099	0.1021	5.8669	23.5420
$\alpha = 2.5$	0.05	29.9937	599.9375	20.0020	7.1430	26.2457
	0.25	5.9692	23.9375	4.0101	7.1124	26.1462
	0.50	2.9411	5.9377	2.0188	7.0253	25.8675
	1.00	1.4000	1.4400	1.0285	6.7708	25.1012
	5.00	0.2137	0.0439	0.2055	6.0633	23.8883
	10.0	0.1019	0.0102	0.1009	6.0152	23.9642
$\alpha = 5.0$	0.05	79.9625	1601.498	20.0281	14.9700	52.3700
	0.25	15.8153	65.4428	4.1379	14.2946	49.4601
	0.50	7.6470	17.2872	2.2606	12.6098	42.4029
	1.00	3.4000	4.8400	1.4235	9.1284	28.8914
	5.00	0.2827	0.0993	0.3513	5.5491	22.1315
	10.0	0.1115	0.0144	0.1298	5.9584	26.4068
$\alpha = 10.0$	0.05	179.90	3613.981	20.0888	36.4314	145.4433
	0.25	35.5076	157.5422	4.4368	31.5520	120.6542
	0.50	17.0588	48.2906	2.8308	22.2211	76.7248
	1.00	7.4000	17.6400	2.3837	10.7061	30.5582
	5.00	0.4206	0.3885	0.9235	4.6814	17.5866
	10.0	0.1307	0.0367	0.2809	6.2247	35.5493
$\alpha = 25$	0.05	479.7126	9726.3384	20.2753	130.0227	711.9315
	0.25	94.5846	506.5505	5.3555	86.2262	413.7612

0.50	45.2941	207.7370	4.5864	39.2306	146.9782
1.00	19.4000	104.0400	5.3628	11.7613	31.1303
5.00	0.8344	2.6829	3.2151	3.9264	12.9181
10.0	0.1884	0.2144	1.1380	6.0984	35.2655

Moment Generating Function

The moment generating function of a random variable X following the NTGL distribution is defined by:

$$\begin{aligned}
 M_X(t) &= \int_0^\infty e^{tx}(x; \alpha, \theta) dx \\
 &= \int_0^\infty e^{tx} \frac{\theta^2}{4 + \theta^2} \left(\theta + \frac{4x^{\alpha-2}\theta^{\alpha-3}}{\Gamma(\alpha-1)} \right) e^{-\theta x} dx \\
 &= \frac{\theta^2}{4 + \theta^2} \int_0^\infty \left(\theta + \frac{4x^{\alpha-2}\theta^{\alpha-3}}{\Gamma(\alpha-1)} \right) e^{-(\theta-t)x} dx \\
 &= \frac{\theta^2}{4 + \theta^2} \left[\int_0^\infty \theta e^{-(\theta-t)x} dx \right. \\
 &\quad \left. + \frac{4\theta^{\alpha-3}}{\Gamma(\alpha-1)} \int_0^\infty x^{\alpha-2} e^{-(\theta-t)x} dx \right]
 \end{aligned}$$

Let $y = (\theta - t)x$

$$\begin{aligned}
 &= \frac{\theta^2}{4 + \theta^2} \left[\theta \int_0^\infty \frac{e^{-y}}{(\theta - t)} dy \right. \\
 &\quad \left. + \frac{4\theta^{\alpha-3}}{\Gamma(\alpha-1)} \int_0^\infty \frac{y^{\alpha-2} e^{-y}}{(\theta - t)^{\alpha-1}} dy \right] \\
 M_X(t) &= \frac{\theta^2}{4 + \theta^2} \left[\frac{\theta}{(\theta - t)} + \frac{4\theta^{\alpha-3}}{(\theta - t)^{\alpha-1}} \right] \tag{4}
 \end{aligned}$$

Reliability Characteristics

In this section, we derive some reliability properties of the NTGL distribution including survival and hazard functions.

3.3.1. Survival Function

The survival function of the NTGL distribution denoted by $S(x)$ is given as follows:

$$\begin{aligned}
 S(x) &= 1 - F(x|\alpha, \theta) \\
 S(x) &= \frac{4 + \theta^2 e^{-\theta x} - 4 \frac{\gamma(\alpha-1, \theta x)}{\Gamma(\alpha-1)}}{4 + \theta^2} \tag{5}
 \end{aligned}$$

Hazard (Failure Rate) Function

The hazard function of the NTGL distribution denoted by $h(x)$ is given as follows:

$$\begin{aligned}
 h(x) &= \frac{f(x|\alpha, \theta)}{S(x)} \\
 h(x) &= \frac{(\theta(x\theta)^{-2+\alpha}(4x^\alpha\theta^\alpha + x^2\theta^4\Gamma(\alpha-1)))}{((\theta^2(x\theta)^\alpha + e^{x\theta}(-4x^\alpha\theta^\alpha + 4(x\theta)^\alpha))\Gamma(\alpha-1) + 4e^{x\theta}x^\alpha\theta^\alpha\Gamma(\alpha-1, x\theta))} \tag{6}
 \end{aligned}$$

For varying values of α and θ Figures 4 and 5, show the shapes of the plots of $S(x)$ and $h(x)$, respectively. Obviously, the NTGL distribution has decreasing and increasing hazard rate functions depending on the values of the parameters.

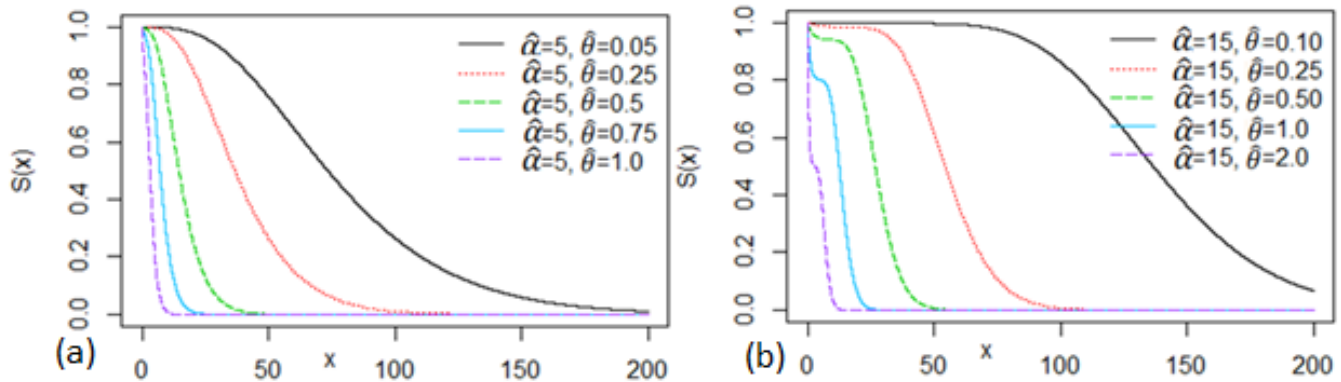


Figure 4: Survival curves of the distribution for some selected values of parameters.

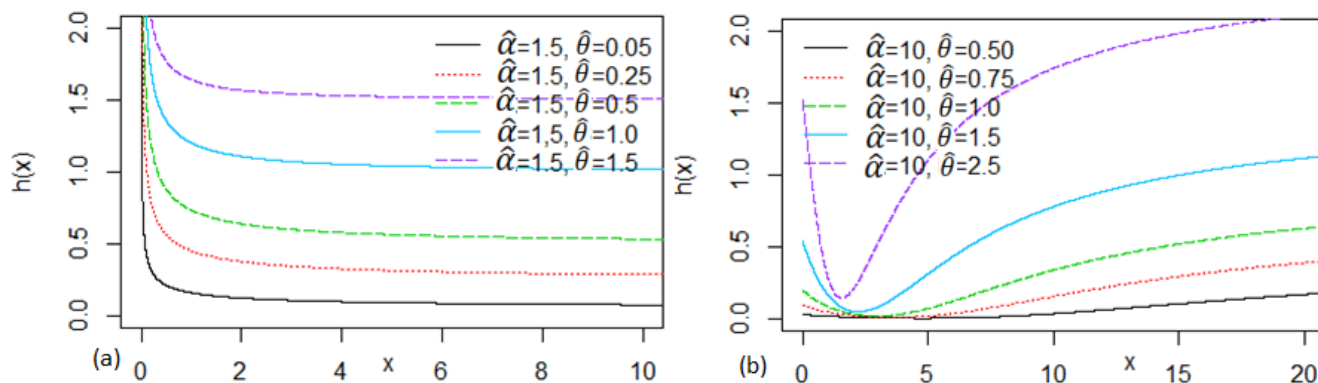


Figure 5: Hazard curves of the distribution for some selected values of the parameters.

Renyi's Entropy

An entropy of a random variable X is a measure of variation of uncertainty [33]. Suppose a continuous random variable X follows a probability with density function $f(x)$, then Renyi's entropy, $R_H(x)$, can be expressed as:

$$R_H(x) = \frac{1}{1-\rho} \log \int_0^{\infty} [f(x|\alpha, \theta)]^{\rho} dx,$$

For the PDF in equation (1) given as:

$$f(x|\alpha, \theta) = \frac{\theta^2}{4 + \theta^2} \left(\theta + \frac{4x^{\alpha-2}\theta^{\alpha-3}}{\Gamma(\alpha-1)} \right) e^{-\theta * x}, \quad x, \alpha, \theta > 0$$

Therefore,

$$\begin{aligned} R_H(x) &= \frac{1}{1-\rho} \log \int_0^{\infty} \left[\frac{\theta^2}{4 + \theta^2} \left(\theta + \frac{4x^{\alpha-2}\theta^{\alpha-3}}{\Gamma(\alpha-1)} \right) e^{-\theta * x} \right]^{\rho} dx \\ &= \frac{1}{1-\rho} \log \left[\left(\frac{\theta^2}{4 + \theta^2} \right)^{\rho} \left(\theta \int_0^{\infty} e^{-\rho\theta x} dx + \frac{4\theta^{\alpha-3}}{\Gamma(\alpha-1)} \int_0^{\infty} x^{\alpha-2} e^{-\rho\theta x} dx \right) \right] \\ &= \frac{1}{1-\rho} \log \left[\left(\frac{\theta^2}{4 + \theta^2} \right)^{\rho} \left(\theta \frac{1}{\rho\theta} + \frac{4\theta^{\alpha-3}}{\Gamma(\alpha-1)} \frac{\Gamma(\alpha-1)}{(\rho\theta)^{\alpha-1}} \right) \right] \\ &= \frac{1}{1-\rho} \log \left[\left(\frac{\theta^2}{4 + \theta^2} \right)^{\rho} \left(\frac{1}{\rho} + \frac{4}{\rho^{\alpha-1}\theta^2} \right) \right] \quad (7) \end{aligned}$$

Order Statistics

Suppose $X_{(1)} \leq X_{(2)} \leq \dots \leq X_{(n)}$ are order observations of X_1, X_2, \dots, X_n taken from the studied distribution then density of the k th order statistic $X_{(k)}$ can be expressed as:

$$f_{X_{(k)}}(x) = \frac{n!}{(k-1)!(n-k)!} f(x|\alpha, \theta) [F(x|\alpha, \theta)]^{k-1} [1 - F(x|\alpha, \theta)]^{n-k} \quad (8)$$

By substituting equations (1) and (2) into (8) we have:

$$\begin{aligned} f_{X_{(k)}}(x) &= \frac{n!}{(k-1)!(n-k)!} \frac{\theta^2}{4 + \theta^2} \left(\theta + \frac{4x^{\alpha-2}\theta^{\alpha-3}}{\Gamma(\alpha-1)} \right) e^{-\theta * x} \left[\frac{(1 - e^{-x\theta})\theta^2 + \frac{4x^{\alpha}\theta^{\alpha}(x\theta)^{-\alpha}(\Gamma(\alpha-1) - \Gamma(\alpha-1, x\theta))}{\Gamma(\alpha-1)}}{4 + \theta^2} \right]^{k-1} \\ &\quad \left[\frac{(1 - e^{-x\theta})\theta^2 + \frac{4x^{\alpha}\theta^{\alpha}(x\theta)^{-\alpha}(\Gamma(\alpha-1) - \Gamma(\alpha-1, x\theta))}{\Gamma(\alpha-1)}}{4 + \theta^2} \right]^{n-k} \end{aligned}$$

The functions of the first and n th order statistics are:

$$\begin{aligned} f_{X_{(1)}}(x) &= \frac{n!}{(k-1)!(n-k)!} \frac{\theta^2}{4 + \theta^2} \left(\theta + \frac{4x^{\alpha-2}\theta^{\alpha-3}}{\Gamma(\alpha-1)} \right) e^{-\theta * x} \left[1 - \frac{(1 - e^{-x\theta})\theta^2 + \frac{4x^{\alpha}\theta^{\alpha}(x\theta)^{-\alpha}(\Gamma(\alpha-1) - \Gamma(\alpha-1, x\theta))}{\Gamma(\alpha-1)}}{4 + \theta^2} \right]^{n-1} \end{aligned}$$

and

$$\begin{aligned} f_{X_{(n)}}(x) &= \frac{n!}{(k-1)!(n-k)!} \frac{\theta^2}{4 + \theta^2} \left(\theta + \frac{4x^{\alpha-2}\theta^{\alpha-3}}{\Gamma(\alpha-1)} \right) e^{-\theta * x} \left[\frac{(1 - e^{-x\theta})\theta^2 + \frac{4x^{\alpha}\theta^{\alpha}(x\theta)^{-\alpha}(\Gamma(\alpha-1) - \Gamma(\alpha-1, x\theta))}{\Gamma(\alpha-1)}}{4 + \theta^2} \right]^{n-1} \end{aligned}$$

Quantile function

The quantile function $Q(p)$ is the inverse of the cdf in (2), defined as:

$$Q(p) = F^{-1}(p)$$

Therefore,

$$\begin{aligned} p &= \frac{(1 - e^{-x\theta})\theta^2 + \frac{4x^{\alpha}\theta^{\alpha}(x\theta)^{-\alpha}(\Gamma(\alpha-1) - \Gamma(\alpha-1, x\theta))}{\Gamma(\alpha-1)}}{4 + \theta^2} \\ p(4 + \theta^2) - \frac{4x^{\alpha}\theta^{\alpha}(x\theta)^{-\alpha}(\Gamma(\alpha-1) - \Gamma(\alpha-1, x\theta))}{\Gamma(\alpha-1)} &= (1 - e^{-x\theta})\theta^2 \end{aligned}$$

This is a complex equation to solve analytically; hence, numerical solution can be obtained. The plot of the quantile

function (at $p = 0.5$) at varying values of α and θ is presented in Figure 6.

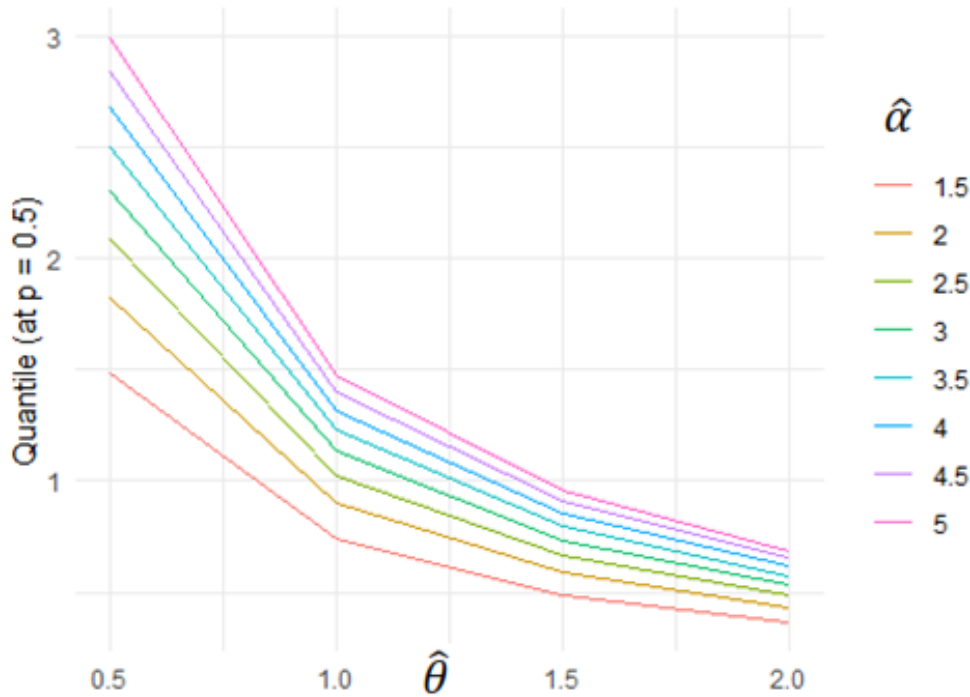


Figure 6: Quantile function (at $p = 0.5$) plot at varying values of α and θ

[IV] PARAMETER ESTIMATION AND SIMULATION STUDY

In this section, we obtain the mathematical expressions of the maximum likelihood estimators (MLEs) of the NTGL distribution (*i.e.*, $\hat{\alpha}_{MLE}, \hat{\theta}_{MLE}$). Besides deriving of the mathematical expression of $\hat{\alpha}_{MLE}$ and $\hat{\theta}_{MLE}$, we also provide a simulation study to assess their performances numerically.

Maximum Likelihood Estimation

Let X_1, X_2, \dots, X_n be a random sample of size n from $f(x|\alpha, \theta)$ of the NTGL distribution defined by (1). In relation to the $f(x|\alpha, \theta)$, the likelihood function $L(\alpha, \theta|x_1, x_2, \dots, x_n)$ of the parameters can be written as

$$L(\alpha, \theta|x_1, x_2, \dots, x_n) = L = \prod_{i=1}^n f(x_i|\alpha, \theta) \quad (9)$$

Using Equation (1) in Equation (9), we have

$$L = \prod_{i=1}^n \frac{\theta^2}{4 + \theta^2} \left(\theta + \frac{4x_i^{\alpha-2}\theta^{\alpha-3}}{\Gamma(\alpha-1)} \right) e^{-\theta x_i} \quad (10)$$

The log likelihood function is obtained by

$$\begin{aligned} \mathcal{L}(\alpha, \theta) = & 2n \log \theta - n \log(4 + \theta^2) \\ & + \sum_{i=1}^n \log \left(\theta + \frac{4x_i^{\alpha-2}\theta^{\alpha-3}}{\Gamma(\alpha-1)} \right) \\ & - \sum_{i=1}^n x_i \theta \quad (11) \end{aligned}$$

The maximum likelihood estimates (MLEs) $\hat{\alpha}$ and $\hat{\theta}$ of the parameters α and θ of NTGL distribution are found by solving the following log-likelihood equation by taking partial derivatives of equation (11) with respect to θ and α and equating to zero, following score equations are obtained as

$$\frac{\partial \mathcal{L}(\alpha, \theta)}{\partial \alpha} = \sum_{i=1}^n \left[\frac{4x_i^{\alpha-2}\theta^{\alpha-3} (x_i^{\alpha-2} \log(x_i) - \frac{\Gamma'(\alpha-1)}{\Gamma(\alpha-1)})}{\left(\theta + \frac{4x_i^{\alpha-2}\theta^{\alpha-3}}{\Gamma(\alpha-1)} \right) \Gamma(\alpha-1)} \right] \quad (12)$$

and

$$\frac{\partial \mathcal{L}(\alpha, \theta)}{\partial \theta} = \sum_{i=1}^n \left[\frac{2\theta}{4 + \theta^2} + \frac{1 + \frac{4x_i^{\alpha-2}(\alpha-3)\theta^{\alpha-3}}{\Gamma(\alpha-1)}}{\theta + \frac{4x_i^{\alpha-2}\theta^{\alpha-3}}{\Gamma(\alpha-1)}} - x_i \right] \quad (13)$$

The Maximum Likelihood estimates $\hat{\alpha}$ and $\hat{\theta}$ of the parameters α and θ respectively, can be obtained by solving iteratively Equations (12) and (13). We solve the non-linear equations numerically because they are not in closed forms, hence, they are complicated to solve algebraically. The R-software [34] was used to solve the equations and obtain the parameters' values.

Simulation Study

In this subsection, we evaluate the behaviors of $\hat{\alpha}_{MLE}$ and $\hat{\theta}_{MLE}$ of the NTGL distribution through a thorough simulation study. The study is carried out by generating random samples (with $N=1000$ iterations), say $n = 50, 100, \dots, 1000$, from NTGL distribution using the inverse cdf approach.

The simulation study was carried out for the combination values $\alpha = 2.5, \theta = 0.5$; $\alpha = 10, \theta = 1.0$ and $\alpha = 10, \theta = 5.0$.

We considered two statistical tools to evaluate the performances of $\hat{\alpha}_{MLE}$ and $\hat{\theta}_{MLE}$. These measures included the bias and mean square error (MSE) with mathematical expressions given, respectively, by

$$MSE(\hat{\theta}_{MLE}) = \frac{1}{N} \sum_{i=1}^N (\hat{\theta}_i - \theta)^2$$

and

$$Bias(\hat{\theta}_{MLE}) = \frac{1}{N} \sum_{i=1}^N (\hat{\theta}_i - \theta)$$

The above evaluation criteria are also computed for $\hat{\alpha}_{MLE}$. The simulation results are presented numerically in Tables 2. From the simulation results of the NTGL distribution, we observed that: as n increases (i.e., as $n \rightarrow \infty$): the estimated values of $\hat{\alpha}_{MLE}$ and $\hat{\theta}_{MLE}$ converge to the true values, indicating stability. Additionally, the MSEs of $\hat{\alpha}_{MLE}$ and $\hat{\theta}_{MLE}$ approach zero. Additionally, the Biases of $\hat{\alpha}_{MLE}$ and $\hat{\theta}_{MLE}$ also decrease to zero.

Table 2: The numerical illustration of the Simulation Study of the NTGL distribution

	n	Parameters	MLEs	MSEs	Biases
$\alpha = 2.5$ $\theta = 0.5$	50	α	2.7318	0.4043	0.2318
		θ	0.5665	0.0348	0.0665
	100	α	2.6063	0.1606	0.1063
		θ	0.5327	0.0152	0.0327
	150	α	2.5791	0.1079	0.0791
		θ	0.5235	0.0106	0.0235
	200	α	2.5444	0.0534	0.0444
		θ	0.5127	0.0055	0.0127
	300	α	2.5295	0.0301	0.0295
		θ	0.5097	0.0032	0.0097
	500	α	2.5161	0.0139	0.0161
		θ	0.5049	0.0017	0.0049
700	α	2.5111	0.0095	0.0111	
	θ	0.5037	0.0011	0.0037	
900	α	2.5083	0.0062	0.0083	
	θ	0.5022	0.0007	0.0022	
1000	α	2.5090	0.0054	0.0090	
	θ	0.5023	0.0006	0.0023	
$\alpha = 10$ $\theta = 1.0$	50	α	10.0769	1.7675	0.0769
		θ	1.0056	0.0193	0.0056
	100	α	10.0091	0.7477	0.0091
		θ	1.0003	0.0083	0.0003
	150	α	10.0234	0.5400	0.0234
		θ	1.0022	0.0060	0.0022
	200	α	10.0500	0.3588	0.0500
		θ	1.0050	0.0041	0.0050
	300	α	9.9873	0.2411	-0.0126
		θ	0.9999	0.0028	-0.0001
	400	α	10.0209	0.1877	0.0209
		θ	1.0010	0.0020	0.0010
500	α	10.0020	0.1300	0.0020	
	θ	1.0007	0.0014	0.0007	
700	α	10.0042	0.0945	0.0042	
	θ	1.0001	0.0010	0.0001	
900	α	9.9927	0.0714	-0.0073	
	θ	0.9995	0.0007	-0.0005	
1000	α	10.0037	0.0664	0.0037	
	θ	1.0001	0.0005	0.0001	
50	α	10.0468	3.2404	0.0468	
	θ	5.0670	0.3193	0.0670	
100	α	10.0063	1.0354	0.0053	
	θ	5.0156	0.1155	0.0156	
150	α	10.0155	0.5395	0.0155	
	θ	5.0105	0.0653	0.0105	

$\alpha = 10$	200	α	10.0113	0.2961	0.0113
		θ	5.0107	0.0397	0.0107
$\theta = 5.0$	300	α	9.9981	0.1141	-0.0019
		θ	4.9939	0.0157	0.0061
	400	α	9.9967	0.0643	-0.0033
		θ	5.0013	0.0090	0.0013
	500	α	9.9993	0.0388	-0.0007
		θ	5.0007	0.0059	0.0007
	700	α	9.9992	0.0091	-0.0008
		θ	5.0004	0.0011	0.0004
	900	α	9.9994	0.0035	-0.0006
		θ	5.0001	0.0002	0.0001
	1000	α	9.999995	0.0016	-5.3×10^{-6}
		θ	4.9995	0.0001	-0.0005

[V] APPLICATION OF REAL DATA ANALYSIS

This section aims to demonstrate the effectiveness of the NTGL distribution using three real data sets. The performance of the NTGL distribution is compared with other competing models, namely: the generalized Lindley distribution (GLD1) by Nadarajah et al. [12], the New Generalized Two Parameter Lindley Distribution (NGTLD) by Ekhoosuehi et al. [35], the quasi-Lindley distribution (QLD) by Shanker and Mishra [13] and the A new generalized Lindley distribution (GLD2) by Abouammoha et al. [14].

Description of the Data Sets

The first data set (onward, it is expressed as Data 1) represents the remission times (in months) of 128 patients who were suffering from bladder cancer. This data set was originally reported by Lee and Wang [36]. The second data set represent the remission times (in months) of 36 bladder cancer patients reported in Hibatullah et al. [37]. The third data set represent the time-to-recovery (in days) of Covid-19 patients at Lagos

state, Nigeria in 2020. It comprises of 553 patients. The secondary data were obtained through the Lagos state ministry of health.

The Model's Selection Tools

In this subsection, we describe the key tools used to evaluate the performance of the NTGL and other competing distributions. The criteria considered in this paper were the Akaike information criteria (AIC), Consistent AIC (CAIC), Bayesian information criteria (BIC), and Hannan–Quinn information criteria (HQIC), with their mathematical expressions detailed as follows:

$$AIC = 2k - 2\mathcal{L},$$

$$CAIC = AIC + \frac{2k(k+1)}{n-k-1},$$

$$BIC = k \log(n) - \mathcal{L}$$

$$HQIC = 2k \log[\log(n)] - 2\mathcal{L}$$

In the formulae of information criteria, the term k represents the model parameter(s), n indicates the sample size, and " \mathcal{L} " represents the Log-likelihood function.

Table 3: The estimated values and model selection values for each data set

Data	Model	$\hat{\alpha}$	$\hat{\theta}$	$-2\log\mathcal{L}$	AIC	CAIC	HQIC	BIC
bladder cancer patients; (n=128)	NTGLD	2.1730	0.1252	826.7385	830.7385	830.8345	833.0561	836.4425
	NGTLD	1.1891	0.1247	826.8288	830.8288	830.9248	833.1463	836.5328
	GLD1	0.7336	0.1648	832.5718	836.5719	836.6679	838.8894	842.2759
	QLD	663.69	0.1069	828.6838	832.6839	832.7799	835.0015	838.3879
	GLD2	1.5890	0.1533	832.3136	836.3136	836.4096	838.6312	842.0177
Bladder cancer dataset (n=36)	NTGLD	4.1345	1.2949	107.1145	111.1145	111.4781	112.2198	114.2815
	NGTLD	2.2531	0.8691	113.2435	117.2435	117.6071	118.3488	120.4105
	GLD1	1.8909	1.0731	107.4763	111.4763	111.84	112.5817	114.6434
	QLD	0.0387	1.0117	108.471	112.471	112.8346	113.5764	115.638
	GLD2	3.1159	1.3135	107.382	111.382	111.7456	112.4874	114.549
*Covid19 data (N=553)	NTGLD	6.4393	0.5053	1651.907	3307.813	3307.835	3311.185	3316.444
	NGTLD	3.6344	0.3099	1701.766	3407.531	3407.553	3410.903	3416.162
	GLD1	2.2552	0.2595	1669.146	3342.292	3342.313	3345.664	3350.922
	QLD	0.0085	0.1954	1708.896	3421.793	3421.815	3425.165	3430.424
	GLD2	3.9631	0.3623	1665.38	3334.760	3334.781	3338.131	3343.390

*Data Source: Lagos state ministry of health

Table 3 compares various models applied to three datasets: remission times of 128 bladder cancer patients, remission times of 36 bladder cancer patients, and time-to-recovery for 553 Covid-19 patients. The models compared are the New Two-Parameter Generalized Lindley Distribution (NTGLD), New Generalized Two Parameter Lindley Distribution (NGTLD), Generalized Lindley Distribution 1 (GLD1), Quasi-Lindley Distribution (QLD), and Generalized Lindley Distribution 2 (GLD2). The performance metrics evaluated include the negative log-likelihood ($-2\log L$), Akaike Information Criterion (AIC), Consistent Akaike Information Criterion (CAIC), Hannan-Quinn Information Criterion (HQIC), and Bayesian Information Criterion (BIC). Lower values of $-2\log L$, AIC, CAIC, HQIC, and BIC indicate a better model fit, and NTGLD consistently achieves the lowest values (bolded) across all datasets. Overall, the NTGL distribution demonstrates superior performance in fitting the datasets compared to other models. It provides more accurate parameter estimates and better fit statistics, making it a robust choice for modeling lifetime datasets.

[VI] CONCLUSION

In this study, we propose a new model called A New Two-Parameter Generalized Lindley Distribution (NTGLD). Its PDF plots demonstrate the flexibility of the NTGLD to model a wide range of behaviors, from sharply peaked distributions to broadly spread, multimodal shapes, depending on the parameter values.

We derive the moments and the moment generating function and other mathematical properties of the distribution. Parameter estimation is estimated using the maximum likelihood method. Simulation results of the NTGL distribution indicate that as the sample size n increases, the estimated values of the parameters α and θ converge to their true values, with mean squared errors (MSEs) and biases approaching zero. This demonstrates the stability and accuracy of the estimators.

From the quantile plot, it is observed that the median quantile decreases as θ increases, with more rapid changes at lower values of θ . Higher values of α consistently result in higher quantiles, highlighting the significant impact of α on the distribution's behavior. Applications to three real datasets, including remission times of bladder cancer patients and time-to-recovery of Covid-19 patients, demonstrate that the NTGL distribution provides better fits compared to other competing models considered.

Although we acknowledge the value of possible extensions such as handling censored data, incorporating Bayesian estimation, regression-based modelling, or offering a public R package, such directions would significantly broaden the scope of this paper. These important developments are reserved for future work. For now, we focus on establishing the theoretical foundations of the NTGLD, consistent with common practice in distributional research.

Conflicts of Interest

The authors declare no conflict of interest.

Data Availability

The third data is available from the corresponding author upon justifiable request.

CRedit authorship contribution statement

Samuel Adewale Aderoju: Conceptualization, investigation, methodology, writing—original draft, and data curation. Kazeem Adesina Dauda: Methodology, Writing—Review & Editing. Julius Babatunde Olaifa: Methodology, Writing—Review & Editing.

Acknowledgment

This research study is supported by TETFUND INSTITUTIONAL BASED RESEARCH (KWASUIBR/CRIT/270921/VOL1/TETF2020/00016) through Kwara State University, Malet. We appreciate the Lagos State Ministry of Health for their cooperation and support in releasing the Covid-19 data (secondary data). We also appreciate Mr. Oludare Arowogbola for his effort in the data collection.

REFERENCES

- [1] G. Warahena-Liyanage, B. Oluyede, T. Moakofi, and W. Sengweni, "The new exponentiated half logistic-Harris-G family of distributions with actuarial measures and applications," *Stats*, vol. 6, pp. 773–801, 2023. doi: 10.3390/stats6030050.
- [2] H. SchÄbe, "Constructing lifetime distributions with bathtub shaped failure rate from DFR distributions," *Microelectronics Reliability*, vol. 34, no. 9, pp. 1501–1508, 1994. doi: 10.1016/0026-2714(94)90458-8.
- [3] M. Chahkandi and M. Ganjali, "On some lifetime distributions with decreasing failure rate," *Comput. Statist. Data Anal.*, vol. 53, no. 12, pp. 4433–4440, 2009. doi: 10.1016/j.csda.2009.06.016.
- [4] K. A. Dauda, "Optimal tuning of random survival forest hyperparameter with an application to liver disease," *Malays. J. Med. Sci.*, vol. 29, no. 6, pp. 67–76, 2022. doi: 10.21315/mjms2022.29.6.7.
- [5] K. A. Dauda, W. B. Yahya, and A. W. Banjoko, "Survival analysis with multivariate adaptive regression splines using Cox-Snell residual," *Ann. Comput. Sci. Ser.*, vol. 13, no. 2, pp. 25–41, 2015.
- [6] A. H. Tolba et al., "A new distribution for modeling data with increasing hazard rate: A case of COVID-19 pandemic and vinyl chloride data," *Sustainability*, vol. 15, art. no. 12782, 2023. doi: 10.3390/su151712782.

- [7] N. L. Johnson, S. Kotz, and N. Balakrishnan, "Beta distributions," in *Continuous Univariate Distributions*, 2nd ed., New York, NY, USA: John Wiley & Sons, 1994, pp. 221–235.
- [8] N. L. Johnson, S. Kotz, and N. Balakrishnan, *Continuous Univariate Distributions*. New York, NY, USA: John Wiley & Sons, 1995, vol. 289.
- [9] F. S. Gomes-Silva, A. Percontini, E. de Brito, M. W. Ramos, R. Venâncio, and G. M. Cordeiro, "The odd Lindley-G family of distributions," *Austrian J. Stat.*, vol. 46, pp. 65–87, 2017. doi: 10.17713/ajs.v46i1.222.
- [10] N. Taketomi, K. Yamamoto, C. Chesneau, and T. Emura, "Parametric distributions for survival and reliability analyses, a review and historical sketch," *Mathematics*, vol. 10, art. no. 3907, 2022. doi: 10.3390/math10203907.
- [11] D. V. Lindley, "Fiducial distributions and Bayes' theorem," *J. R. Stat. Soc. Ser. B*, vol. 20, pp. 102–107, 1958. doi: 10.1111/j.2517-6161.1958.tb00278.x.
- [12] H. Zakerzadeh and A. Dolati, "Generalized Lindley distribution," *J. Math. Ext.*, vol. 3, pp. 13–25, 2009. doi: 10.4236/ojs.2021.113022.
- [13] B. O. Oluyede and T. Yang, "A new class of generalized Lindley distributions with applications," *J. Stat. Comput. Simul.*, vol. 85, no. 10, pp. 2072–2100, 2015. doi: 10.1080/00949655.2014.917308.
- [14] S. Nadarajah, H. S. Bakouch, and R. Tahmasbi, "A generalized Lindley distribution," *Sankhya B*, vol. 73, pp. 331–359, 2011. doi: 10.1007/s13571-011-0025-9.
- [15] R. Shanker and A. Mishra, "A quasi-Lindley distribution," *Afr. J. Math. Comput. Sci. Res.*, vol. 6, no. 4, pp. 64–71, 2013. doi: 10.5897/AJMCSR12.067.
- [16] A. M. Abouammoh, A. M. Alshangiti, and I. E. Ragab, "A new generalized Lindley distribution," *J. Stat. Comput. Simul.*, 2015. doi: 10.1080/00949655.2014.995101.
- [17] N. H. Al-Noor and N. K. Assi, "Rayleigh-Rayleigh distribution: Properties and applications," *J. Phys.: Conf. Ser.*, vol. 1591, art. no. 012038, 2020. doi: 10.1088/1742-6596/1591/1/012038.
- [18] K. K. Shukla, "Pranav distribution with properties and its applications," *Biometrics Biostat. Int. J.*, vol. 7, no. 3, pp. 244–254, 2018. doi: 10.15406/bbij.2018.07.00215.
- [19] S. Aderoju, "Samade probability distribution: Its properties and application to real lifetime data," *Asian J. Probab. Stat.*, vol. 14, no. 1, pp. 1–11, 2021. doi: 10.9734/ajpas/2021/v14i130317.
- [20] S. A. Aderoju and O. Babaniyi, "Power Samade distribution: Its properties and application to real lifetime data," *Niger. J. Sci. Environ.*, vol. 21, no. 1, pp. 237–248, 2023.
- [21] R. Elangovan and K. Manivasagan, "A new generalization of Samade distribution with properties and its applications in medical sciences," *Strad Res.*, vol. 10, no. 6, 2023. doi: 10.37896/sr10.6/048.
- [22] S. Aryuyuen, I. Thaimsorn, and U. Tonggumnead, "Bayesian inference for a new negative binomial-Samade model for time series data counts with its properties and applications," *WSEAS Trans. Math.*, 2023. doi: 10.37394/23206.2023.22.65.
- [23] S. A. Aderoju, I. Adeniyi, J. B. Olaifa, and A. Olaosebikan, "On Poisson-Samade distribution: Its applications in modelling count data," *Earthline J. Math. Sci.*, vol. 12, no. 2, pp. 255–270, 2023. doi: 10.34198/ejms.12223.255270.
- [24] B. Hosseini, M. Afshari, M. Alizadeh, and A. Afify, "A new weighted-Lindley distribution: Properties, classical and Bayesian estimation with an application," *Pak. J. Stat. Oper. Res.*, vol. 18, no. 4, pp. 1049–1066, 2022. doi: 10.18187/pjsor.v18i4.4106.
- [25] B. Meriem et al., "The power XLindley distribution: Statistical inference, fuzzy reliability, and COVID-19 application," *J. Funct. Spaces*, vol. 2023, art. no. 9818094, 2023. doi: 10.1155/2023/9818094.
- [26] S. A. Aderoju and E. T. Jolayemi, "Power Hamza distribution and its applications to model survival time," *J. Niger. Stat. Assoc.*, vol. 34, pp. 1–10, 2022.
- [27] N. I. Aleshinloye, S. A. Aderoju, A. A. Abiodun, and B. L. Taiwo, "A new generalized gamma-Weibull distribution and its applications," *Al-Bahir J. Eng. Pure Sci.*, vol. 2, no. 2, pp. 1–9, 2023. doi: 10.55810/2313-0083.1021.
- [28] S. A. Aderoju and I. Adeniyi, "On power generalized Akash distribution with properties and applications," *J. Stat. Model. Anal.*, vol. 4, no. 1, 2023. doi: 10.22452/josma.vol4no1.1.
- [29] Y. A. Tashkandy, M. E. Bakr, S. A. Benchiha et al., "Power modified XLindley distribution: Statistical properties and applications," *Sci. Rep.*, vol. 14, art. no. 20262, 2024. doi: 10.1038/s41598-024-69884-5.
- [30] A. M. Gemeay et al., "Modified XLindley distribution: Properties, estimation, and applications," *AIP Adv.*, 2023. doi: 10.1063/5.0172056.
- [31] S. A. Aderoju, N. I. Aleshinloye, B. L. Taiwo, and B. I. Sanni, "A new lifetime distribution and its application to cancer data," *J. Biostat. Epidemiol.*, vol. 9, no. 4, pp. 451–460, 2024. doi: 10.18502/jbe.v9i4.16670.

- [32] B. S. Everitt and D. J. Hand, "Mixtures of normal distributions," in *Finite Mixture Distributions*, Dordrecht: Springer, 1981, pp. 25–57. doi: 10.1007/978-94-009-5897-5_2.
- [33] A. Renyi, "On measures of entropy and information," in *Proc. Fourth Berkeley Symp. Math. Statist. Prob.*, vol. 1, pp. 547–561, 1961.
- [34] R Core Team, *R: A Language and Environment for Statistical Computing*, Vienna, Austria: R Foundation for Statistical Computing, 2023. [Online]. Available: <https://www.R-project.org/>.
- [35] N. Ekhsuehi, F. Opono, and F. Odobaire, "A new generalized two parameter Lindley distribution," *J. Data Sci.*, vol. 16, no. 3, pp. 549–566, 2018. doi: 10.6339/JDS.201807_16(3).0006.
- [36] E. T. Lee and J. Wang, *Statistical Methods for Survival Data Analysis*. New York, NY, USA: Wiley, 2003.
- [37] R. Hibatullah, Y. Widyaningsih, and S. Abdullah, "Marshall-Olkin extended power Lindley distribution with application," *J. Riset Apl. Mat.*, vol. 2, no. 2, pp. 84–92, 2018. doi: 10.26740/jram.v2n2.p84-92.